Check for updates

QbD-optimized HA–Pluronic nanomicelles for the targeted repurposing of tofacitinib in breast cancer

Suchita Waghmare, [ID] *[a] Rohini Palekar, [ID] [a] Pratiksha Bramhe, [ID] [a] Nilesh Rarokar [ID] [b] and Pramod Khedekar [ID] [a,c]

Tofacitinib, a Janus kinase (JAK) inhibitor clinically approved for rheumatoid arthritis, holds significant potential for repurposing in breast cancer therapy due to its ability to suppress the oncogenic STAT3 signaling pathway; however, its therapeutic application is hindered by poor aqueous solubility, rapid systemic clearance, and non-specific distribution. To address these limitations, this study aimed to develop hyaluronic acid (HA)-decorated Pluronic F127 (PF127) micelles to enhance the solubility, bioavailability, and targeted delivery of Tofacitinib to CD44-overexpressing breast cancer cells. A Quality by Design (QbD) approach utilizing a Box–Behnken design (BBD) was employed to systematically optimize critical process parameters—drug-to-polymer ratio, polymer concentration, and stirring temperature—to minimize particle size and polydispersity index (PDI) while maximizing entrapment efficiency. The optimized micelles exhibited a uniform particle size of 159.2 ± 3.8 nm, a narrow PDI of 0.221, a high entrapment efficiency of 91.14%, and a negative zeta potential of −24.6 mV, ensuring colloidal stability. *In vitro* evaluation demonstrated a sustained, diffusion-controlled drug release profile and significantly enhanced cytotoxicity against MCF-7 breast cancer cells (IC_{50} 14.2 µg mL^{-1}) compared to the free drug (IC_{50} 46.8 µg mL^{-1}), attributed to CD44-mediated cellular uptake. Furthermore, *in vivo* pharmacokinetic analysis in Wistar rats revealed a 4.3-fold increase in oral bioavailability and a prolonged elimination half-life compared to free Tofacitinib, while histopathological studies confirmed the formulation's biocompatibility and safety in major organs. These findings collectively support the viability of the QbD-optimized HA–PF127 micellar system as a promising nanocarrier platform for the effective oral repurposing of Tofacitinib in breast cancer treatment.

1. Introduction

It is considered that breast cancer is the most frequently diagnosed malignancy and a leading cause of cancer-related mortality among women worldwide, accounting for an estimated 2.3 million new cases and 670 000 deaths in 2022.[1] Although much progress has been made in molecular diagnostics and targeted therapies, systemic toxicity, multidrug resistance, and poor solubility of anticancer drugs remain major obstacles to the therapeutic management of breast cancer. The challenges mentioned above necessitate nanotechnology-based delivery systems that can improve solubility and pharmacokinetic pro-

files while achieving tumor-specific targeting with reduced adverse effects.[2]

Among the nanocarrier systems, PMs have emerged as one of the versatile platforms for delivering anticancer drugs owing to their amphiphilic structure, biocompatibility, and high drug-loading ability. They self-assemble in aqueous media, forming a hydrophobic core that allows the encapsulation of poorly water-soluble drugs and a hydrophilic corona that provides colloidal stability.[3] Pluronic F127, an FDA-approved tri-block copolymer of PEO and PPO, has been widely used for the delivery of drugs because it is considered safe and promotes the formation of stable micellar systems. However, passive delivery only is usually not sufficient for selective tumor targeting.[4]

To overcome this limitation, hyaluronic acid (HA), a naturally occurring glycosaminoglycan, has been broadly introduced into nanocarriers with the purpose of increasing their biological recognition and cellular internalization *via* CD44 receptor-mediated endocytosis.[5] CD44 is overexpressed on many breast

[a]Department of Pharmaceutical Sciences, Rashtrasant Tukadoji Maharaj Nagpur University, Nagpur, Maharashtra, 440033, India.
E-mail: suchitawaghmare26@gmail.com
[b]Sharda Institute of Pharmaceutical Science and Research Centre, Goregaon, Gondia, India
[c]Nagpur College of Pharmacy, Wanadongari, Hingna, India

cancer cells, and HA-based nanocarriers have demonstrated superior tumor penetration and accumulation when compared with non-targeted systems.[6] As an example, HA-decorated doxorubicin nanoplatforms significantly enhanced cytotoxicity and reduced resistance in models of breast carcinoma, confirming the potential of HA-assisted targeting in nanomedicine.[7] Along the same line, HA-functionalized polymeric micelles increased the therapeutic index of paclitaxel through an improved biodistribution and sustained drug release.[8]

The JAK/STAT pathway, especially STAT3, is considered a key oncogenic driver in the progression of breast cancer, regulating cell survival, proliferation, and metastasis. Poor prognosis and chemoresistance have been associated with sustained activation of STAT3. Targeting this pathway thus represents an effective therapeutic approach.[9] Tofacitinib, a selective JAK inhibitor approved for rheumatoid arthritis, has recently received attention because of its ability to suppress STAT3 phosphorylation and its downstream oncogenic signaling.[10] Several recent studies have proposed its repurposing for solid tumors, including breast and pancreatic cancers, given its dual action on the inflammatory and proliferative signaling pathways. However, poor aqueous solubility and low bioavailability of the drug require a nanocarrier-based approach to achieve efficient tumor-specific delivery.[11]

In the present study, hyaluronic acid (HA)–assisted Pluronic F127 micelles were rationally developed and optimized for the encapsulation and delivery of tofacitinib as a repurposed STAT3 inhibitor for breast cancer therapy. A Quality by Design (QbD)–based optimization strategy employing a Box–Behnken experimental design was implemented to systematically investigate the influence of critical formulation and process variables, including drug-to-polymer ratio, polymer concentration, and stirring temperature, on key quality attributes such as particle size and entrapment efficiency. This statistically driven approach enables predictive control of formulation performance, ensures batch-to-batch reproducibility, and aligns the development process with ICH Q8–Q11 regulatory guidelines.

The optimized micellar system was comprehensively characterized for physicochemical properties, morphology, and *in vitro* drug release behaviour, followed by evaluation of its cytotoxic potential against breast cancer cell lines and *in vivo* pharmacokinetic performance. Importantly, the selection of the oral route was guided by the clinically established oral administration of tofacitinib and the increasing reliance on chronic oral targeted therapies in breast cancer management. However, the application of tofacitinib in oncology is limited by poor aqueous solubility, low oral bioavailability, and rapid systemic clearance, which necessitate a nanocarrier-based delivery strategy.

Although HA-decorated Pluronic micellar systems have been reported previously, most studies rely on empirical formulation approaches, focus on conventional cytotoxic agents, and are primarily designed for parenteral administration. In contrast, the present work uniquely integrates a regulatory-aligned QbD framework, HA-mediated active targeting, and oral nanodelivery to enable the repurposing of tofacitinib, a clinically approved JAK inhibitor, for breast cancer therapy. By

establishing a validated design space and control strategy and demonstrating enhanced oral bioavailability and sustained systemic exposure, this study advances HA–Pluronic micelles from a proof-of-concept nanocarrier toward a rational, scalable, and translational oral nanomedicine platform for targeted breast cancer treatment.

2. Materials

Hyaluronic acid (molecular weight $1.5–1.8 \times 10^6$ Da) was procured from BLD Pharma Pvt. Ltd, India. Pluronic F127 (poloxamer 407) was obtained from Himedia Laboratories Pvt. Ltd, Mumbai, India. Tofacitinib was provided as a gift sample by Dr Reddy's Laboratories, Hyderabad, India. Analytical-grade dimethyl sulfoxide (DMSO) and *N,N*-dimethylaminopyridine (DMAP) were purchased from Merck Specialties Pvt. Ltd, India, while carbonyldiimidazole (CDI) was obtained from SRL Pharma, Mumbai, India. All other solvents and reagents used in this study were of analytical grade and used without further purification. Milli-Q ultrapure water was used for all experimental procedures.

3. Materials and methods

3.1. Preformulation studies

These studies were conducted to understand the physical and chemical properties of Tofacitinib, its interaction with HA, and the properties of Pluronic F127 excipients. Such studies form an important part of ensuring chemical stability, identifying potential interactions, and screening for suitable polymers toward micellar formulation.[11]

3.1.1. Differential scanning calorimetry (DSC). The thermal behavior of tofacitinib (TF), each excipient, and their respective physical mixtures was analyzed by Mettler Toledo DSC 3+. Accurately weighted 2–5 mg samples were sealed in aluminum pans and heated from 30 °C to 300 °C under a nitrogen purge of 50 mL min^{-1} at a heating rate of 10 °C min^{-1}. Thermograms were interrogated for shifts in melting endotherms/peaks to infer potential interactions between the drug and excipients.[12]

3.1.2. Fourier transform infrared spectroscopy (FTIR). Chemical compatibility of TF with HA and with Pluronic F127 was evaluated by means of FTIR spectroscopy using a Shimadzu IR Affinity-1S spectrophotometer. Spectra of pure components and their physical mixtures were recorded between 4000 and 400 cm^{-1}, utilizing the KBr pellet method. The spectra thus obtained were compared with each other in order to observe any change in the characteristic peaks of functional groups, which could indicate chemical incompatibility.[13]

3.2. Design space of QbD for development of HA–Pluronic–tofacitinib micelles

A QbD framework was systematically executed to rationally develop Hyaluronic acid–Pluronic F127–Tofacitinib (HA–

PF127–TF) micellar formulation. In the context of this study, QbD is a scientific approach with the purpose of ensuring the robustness of the formulation, improving process understanding, and assuring regulatory compliance by the systematic evaluation of formulation and process variables. This framework consisted of defining quality target product profile, identification of critical quality attributes, critical material attributes, and critical process parameters, structured risk analysis using failure mode and effects analysis, and determination of a statistically validated design space and control strategy.[14]

3.2.1. Quality target product profile (QTPP) definition. QTPP outlines the desired quality characteristics of the final micellar formulation that would be necessary to ensure therapeutic efficacy and patient safety. This was then used to identify the CQAs and further develop the risk analysis. The QTPP for HA–PF127–TFB micelles was defined according to the intended route of administration, *i.e.*, oral; intended therapeutic purpose, *i.e.*, STAT3 inhibition in breast cancer; target performance parameters, *i.e.*, nanoscale size, uniformity, stability, and sustained drug release.[15]

3.2.2. Identification of critical quality attributes (CQAs), critical material attributes (CMAs), and critical process parameters (CPPs). CQAs were defined as measurable physicochemical attributes that directly impact product performance and stability, including particle size, PDI, entrapment efficiency (%), zeta potential, and drug release profile. Potential influencing factors (CMAs and CPPs) were identified from previous experimental evidence and literature on Pluronic-based micellar systems. Table 1 lists the aforementioned attributes and parameters, including their qualitative impact on CQAs. The critical CMAs included the drug-to-polymer ratio, concentration of Pluronic F127, and amount of Hyaluronic acid added; major CPPs were stirring temperature, hydration volume, and sonication time.[16] An integrated summary of the Quality Target Product Profile (QTPP), Critical Quality Attributes (CQAs), Critical Material Attributes (CMAs), and Critical Process Parameters (CPPs) used in the QbD-driven development of HA–Pluronic–Tofacitinib micelles is presented in Table 1.

3.2.3. Risk assessment (FMEA and probability–impact matrix). An extensive FMEA was performed to quantify the

Table 1 Integrated quality by design (QbD) framework for HA–Pluronic–Tofacitinib micelles, summarizing the quality target product profile (QTPP), critical quality attributes (CQAs), critical material attributes (CMAs), and critical process parameters (CPPs)

QbD element	Attribute/parameter	Target/range	Scientific rationale	Criticality/control strategy
QTPP	Intended use	Targeted delivery of tofacitinib for STAT3 inhibition in breast cancer	Enables repurposing of a clinically approved JAK inhibitor for oncology *via* nanocarrier-based delivery	High
	Dosage form	Nanosized polymeric micelles (HA–Pluronic system)	Improves solubility, stability, and controlled release of poorly soluble drug	High
	Route of administration	Oral	Non-invasive, patient-friendly route aligned with existing clinical use of tofacitinib	Medium
	Stability	≥6 months at 25 ± 2 °C	Ensures reproducibility and translational feasibility	High
CQA	Particle size (nm)	100–200 nm	Governs oral absorption, biodistribution, and tumor accumulation	High; controlled *via* design space
	Polydispersity index (PDI)	<0.30	Ensures formulation homogeneity and consistent pharmacokinetics	High; controlled by mixing and polymer concentration
	Zeta potential (mV)	−25 to −35	Provides colloidal stability and reduces aggregation	High; controlled by HA concentration and pH
	Entrapment efficiency (%)	>80	Ensures adequate drug incorporation and dose delivery	High; optimized *via* polymer ratio and temperature
	Drug loading (%)	10–20	Balances dose strength and micelle stability	Medium; controlled by drug-to-polymer ratio
	In vitro drug release	Sustained, up to 48 h	Maintains prolonged systemic exposure and reduces dosing frequency	High; governed by core–shell architecture
CMA	Drug-to-polymer ratio	1 : 10–1 : 20 (w/w)	Controls micellization, encapsulation efficiency, and size	High impact on CQAs
	PF127 concentration (% w/v)	0.5–1.5	Influences micelle stability and size distribution	Moderate to high
	HA concentration (% w/v)	0.1	Enables CD44 targeting and surface charge modulation	Moderate
CPP	Stirring temperature (°C)	30–50	Affects polymer self-assembly and drug entrapment	High; selected *via* FMEA and BBD
	Stirring speed (rpm)	Fixed	Ensures uniform film formation and hydration	Low
	Sonication time	Fixed (3 min)	Reduces particle size and polydispersity	Low
	Hydration medium & pH	PBS, pH 6.8	Mimics physiological conditions for oral delivery	Moderate

potential risk for each CMA and CPP on each CQA. Each parameter was scored for S, O, and D based on a scale of 1–10. RPN was calculated as RPN = $S \times O \times D$. Parameters with RPN values ≥150 were classified as highrisk and selected for statistical optimization.

Results of the FMEA (SI Table S1) identified the three most critical parameters that can affect micellar size and encapsulation efficiency: drug-to-polymer ratio, Pluronic F127 concentration, and stirring temperature. Thus, these variables were selected for experimental modeling *via* a Box–Behnken design based on this analysis.[17]

In the present study, an RPN threshold of ≥150 was selected to classify formulation and process variables as high-risk. This cut-off was chosen based on established pharmaceutical QbD practices, where parameters exhibiting a combination of high severity, high probability of occurrence, and low detectability are considered most likely to impact critical quality attributes. The selected threshold ensured focused prioritization of variables with the greatest potential to influence micellar size distribution and entrapment efficiency, while avoiding unnecessary inclusion of low-risk parameters that could compromise model robustness and interpretability. Variables exceeding this threshold were therefore subjected to further statistical optimization using the Box–Behnken design.

3.2.4. Experimental design and design space establishment. Using Design-Expert® software, Version 13, Stat-Ease Inc., USA, a 3^3 BBD was developed to assess the quantitative impact of selected variables. Independent factors were therefore coded: A – drug-to-polymer ratio; B – Pluronic F127 concentration, and C – stirring temperature. Dependent responses were Y_1 – particle size, nm; Y_2 – PDI; Y_3 – entrapment efficiency, %. Thus, 17 experimental runs were generated and analyzed by RSM.

Relationships among the variables were established by fitting a polynomial regression model, and the adequacy of the fitted model was then checked using ANOVA. Contour plots and 3D response surfaces were used to visualize variable interactions and predict optimum conditions. Design space was defined as a region that would provide robust CQAs within the target range. The desirability function approach was used to choose the optimal formulation based on the criteria of minimum particle size and PDI, and maximum entrapment efficiency.[18]

3.2.5. Control strategy and model validation. All optimized parameters were experimentally validated to confirm predictive accuracy. Observed values of CQAs were compared with the predicted values, and the calculation of percentage prediction error was performed. These results showed that all experimental data fell within a 95% confidence interval, confirming the robustness of the developed design space.

Thus, the established QbD framework provided a structured, risk-based, and statistically driven methodology for the development of HA–Pluronic micelles of TF, ensuring product reproducibility with consistent performance.

Beyond laboratory-scale validation, the established control strategy provides a framework for scalable and reproducible

manufacturing of HA–Pluronic–Tofacitinib micelles. The critical process parameters identified through QbD analysis—namely drug-to-polymer ratio, Pluronic F127 concentration, and stirring temperature—are defined within a validated design space that can be directly translated to larger-scale processing. During scale-up, these parameters may be controlled through predefined operating ranges, real-time monitoring of process temperature and mixing conditions, and in-process particle size assessment as part of process analytical technology (PAT) tools. Adherence to the defined design space allows for flexibility in scale without compromising critical quality attributes, in accordance with ICH Q8 and Q10 guidelines, thereby ensuring consistent product quality and regulatory compliance.

3.3 Formulation and optimization of tofacitinib-loaded HA–Pluronic micelles

The HA–PF127–TF micelles were then prepared by the solvent evaporation and thin-film hydration technique, followed by QbD-based optimization, as established in the preceding section. This approach allowed the particle size, entrapment efficiency, and homogeneity of the micelles to be precisely controlled *via* a systematic variation of key formulation parameters.[19]

3.3.1. Preparation of Pluronic–tofacitinib micelles. Accordingly, accurately weighed quantities of PF127 and TF were dissolved in 10 mL of methanol–chloroform mixture in a 2 : 1 v/v ratio to obtain a clear organic solution. The organic solvent mixture was removed by evaporation under reduced pressure using a Buchi R-300 rotary evaporator at 40 °C and 120 rpm until a uniform thin film formed on the wall of the flask. The film was further dried under vacuum for 2 hours to remove residual solvent. The dried film was subsequently hydrated with 10 mL of phosphate-buffered saline, PBS, pH 6.8, at 37 °C, followed by gentle stirring at 300 rpm for 30 min to obtain self-assembled Pluronic micelles encapsulating TF.[20]

3.3.2. Hyaluronic acid incorporation. For the preparation of HA-assisted micelles, the pre-formed PF127–TF micelles were blended with an aqueous HA solution (0.1% w/v) under continuous stirring at 300 rpm for 1 hour. The hydrophilic HA chains are electrostatically associated with the micelle corona, resulting in HA–PF127–TF micelles with enhanced surface charge and improved biological compatibility (Fig. 1). The formulation was filtered through a 0.22 μm membrane filter to remove any aggregates and stored at 4 °C for further studies. The structural organization and targeting mechanism of the HA–Pluronic–Tofacitinib nanomicelles are depicted schematically in Fig. 2.

3.3.3. Optimization using Box–Behnken design. In accordance with the FMEA analysis done in Section 3.2, three independent variables, namely, drug-to-polymer ratio (A), Pluronic F127 concentration (B), and stirring temperature (C), were optimized through Box–Behnken design (3^3) using Design-Expert® 13 software, Stat-Ease Inc., USA. Particle size, Y_1; polydispersity index, Y_2; and entrapment efficiency, Y_3, were dependent variables or responses.
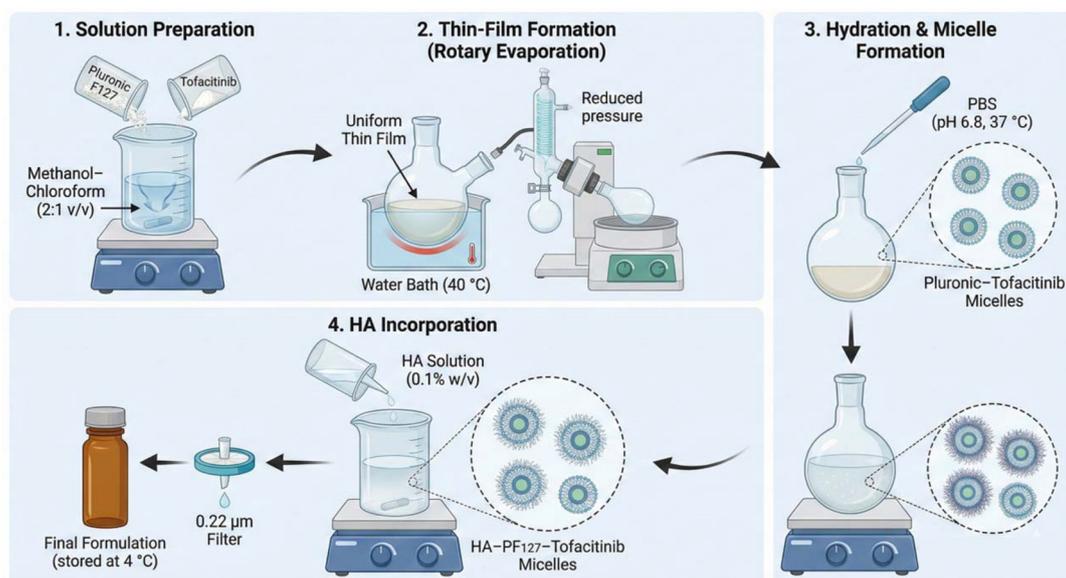
Fig. 1 Schematic illustration of the preparation of Hyaluronic Acid (HA)−modified Pluronic F127 micelles loaded with Tofacitinib.
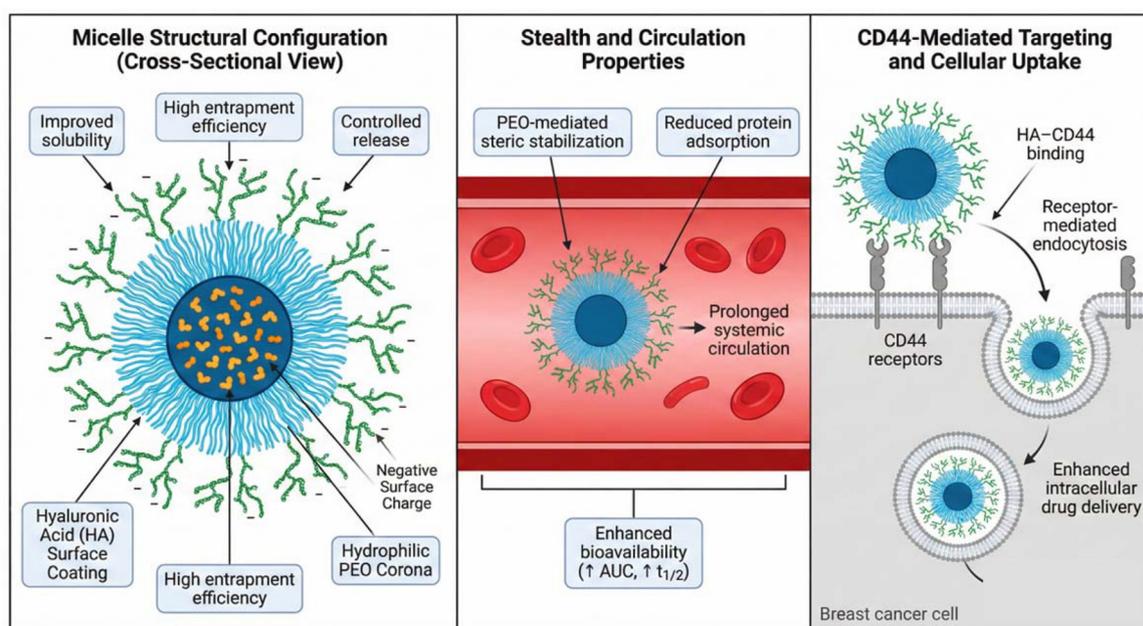

Fig. 2 Schematic illustration of HA-coated Pluronic F127 micelles encapsulating tofacitinib, showing hydrophobic core formation, PEO-mediated stealth properties, and HA-driven CD44 receptor targeting in breast cancer cells.

To investigate the interactive effects between the independent factors and the responses, seventeen experimental runs were generated. Table 2 illustrates the experimental matrix. The responses obtained were fitted to a second order polynomial equation, and adequacy of the model was checked through ANOVA.

The response surface and contour plots were analyzed to identify the region of optimal formulation. The desirability function approach was employed to find the optimum conditions which would provide minimum particle size and PDI, along with maximum entrapment efficiency. Under such predicted conditions, the optimized formulation was prepared and experimental results were compared with the predicted values to verify model predictability.[21]

3.3.4. Selection and validation of optimized formulation. The physicochemical properties of the optimized HA–PF127–

Table 2 Comprehensive QbD table: independent variables, responses, and fixed parameters for HA–Pluronic–Tofacitinib micelles

Category	Parameter	Code	Low level (−1)	Medium level (0)	High level (+1)	Experimental range/units	Optimization goal	Scientific justification
Independent variable	A: drug-to-polymer ratio (Tofacitinib : PF127)	A	01 : 10	01 : 15	01 : 20	0.1 to 0.3 (w/w) equivalent	—	Higher polymer proportion improves micellization and EE up to an optimal limit (beyond 1 : 20 viscosity increases).
	B: PF127 concentration (% w/v)	B	0.5	1	1.5	0.5 to 1.5%	—	Determines micelle density and stability; excess polymer causes high viscosity and potential aggregation.
	C: stirring temperature (°C)	C	30	40	50	30 to 50 °C	—	Temperature modulates micellization; optimal assembly occurs near 40 °C, above which polymer degradation risk increases.
Dependent response	Y_1: particle size (nm)	Y_1	—	—	—	—	Minimize	Nanometer-scale micelles (<200 nm) ensure enhanced permeation and retention (EPR) effect in tumors.
	Y_2: polydispersity index (PDI)	Y_2	—	—	—	—	Minimize	Reflects micelle uniformity and formulation stability.
	Y_3: entrapment efficiency (%)	Y_3	—	—	—	—	Maximize	Ensures sufficient Tofacitinib incorporation for therapeutic efficacy.
Fixed parameter	Hydration volume	—	—	—	—	10 mL	—	Maintains consistent micelle concentration and reproducibility.
	Stirring speed	—	—	—	—	400 rpm	—	Ensures uniform film formation during solvent evaporation.
	Stirring duration	—	—	—	—	30 min	—	Provides adequate polymer and drug dispersion.
	Sonication time	—	—	—	—	3 min (30% amplitude)	—	Reduces micelle size while avoiding rupture.
	Hydration medium	—	—	—	—	PBS (pH 6.8)	—	Mimics physiological conditions for oral delivery.
	HA concentration	—	—	—	—	0.1% w/v	—	Enables effective surface association for CD44 targeting.
	Storage temperature	—	—	—	—	4 °C	—	Preserves micelle integrity prior to characterization.

TF micelle formulation fell within the predefined design space. To validate the model-predicted values, triplicate preparations of the optimized formulation were prepared under optimized conditions and particle size, PDI, and entrapment efficiency were determined. Percentage prediction error between observed and predicted values was calculated to verify the reliability of QbD model. Optimized micellar dispersion was stored at 4 °C in amber vials until further characterization and evaluation.

3.4. Characterization of optimized micelles

The optimized HA–PF127–TF micelles were characterized comprehensively using physicochemical and morphological techniques to confirm successful formulation, stability, and suitability for biological evaluation. All analyses were performed in triplicate under controlled laboratory conditions unless stated otherwise.[22]

3.4.1. Particle size, polydispersity index (PDI), and zeta potential. Then, the micellar formulation was characterized for average particle size distribution using DLS with a Malvern Zetasizer Nano ZS90 (Malvern Instruments, UK) at 25 ± 1 °C. Before measurement, the micellar dispersion was diluted tenfold with double-distilled water in order to avoid the multiple scattering effect. Hydrodynamic diameter (Z-average) and PDI were recorded as indices of size uniformity. Zeta potential was measured in a disposable folded capillary cell using laser Doppler micro-electrophoresis in order to assess the electrokinetic stability of the micelles. Each measurement was carried out in triplicate and the mean value was recorded for analysis.[23]

3.4.2. Entrapment efficiency (EE%) and drug loading (DL%). Entrapment efficiency and drug loading were determined by the ultracentrifugation method. A known volume of micellar suspension (2 mL) was centrifuged at 15 000 rpm for 30 min at 4 °C using a Remi C-24 BL centrifuge in order to separate the unentrapped TF. Then, the supernatant collected, sutaibly diluted and analyzed for free drug content by HPLC under sutaible conditions. Total and entrapped drug content

were calculated, and EE% and DL% were determined using standard mathematical relationships. All the experiments were performed in triplicate to ensure accuracy.

3.4.3. Morphological analysis. TEM and SEM were employed to visualize the surface morphology and particle structure of the optimized micelles, respectively. For TEM analysis, a drop of the diluted micellar dispersion was placed on a carbon-coated copper grid, negatively stained with 1% phosphotungstic acid, air-dried, and observed in a JEOL JEM-2100 electron microscope at 120 kV. In SEM imaging, the lyophilized micelles were mounted on an aluminum stub, sputter-coated with gold using a Quorum SC7620 sputter coater, and analyzed with a Hitachi S-4800 field emission SEM to visualize the surface topology and morphology.[24]

3.4.4. *In vitro* drug release study. To evaluate the *in vitro* release property and controlled-release behaviour of micelles, the dialysis bag diffusion technique was employed. A pre-soaked dialysis membrane (with a molecular weight cut-off of 12 000–14 000 Da) containing 2 mL of micellar dispersion (equivalent to 2 mg of Tofacitinib) was inserted into 100 mL of phosphate buffer (pH 7.4), maintained at 37 ± 0.5 °C under continuous magnetic stirring at 100 rpm. At pre-calculated time intervals, 2 mL samples were withdrawn and replaced with an equivalent amount of fresh buffer to maintain sink conditions. The samples were assayed by HPLC at 287 nm. Zero-order, first-order, Higuchi, and Korsmeyer-Peppas equations were employed for the release kinetics modelling, and regression analysis was utilized to identify the most appropriate mechanism that best describes the release.[25]

3.4.5. Stability studies. Physical stability testing of the optimized micellar formulation was performed by keeping the lyophilized samples in amber glass vials at two storage conditions: 4 ± 2 °C (refrigerated) and 25 ± 2 °C/$60 \pm 5\%$ RH (ambient) for a period of three months. The samples were periodically analyzed for particle size, PDI, zeta potential, and entrapment efficiency during this storage period to monitor any physicochemical changes. Stability testing was conducted following ICH Q1A (R2) guidelines.[26]

3.5. *In vitro* cytotoxicity (MTT assay)

The MTT colorimetric assay was conducted to assess the cytotoxic potential of the optimized HA–PF127–TF micelles against the MCF-7 human breast cancer cell line. In this experiment, the antiproliferative activity of the optimized micellar formulation was compared with that of free Tofacitinib and non-HA-modified micelles. All procedures were performed under aseptic conditions, and each experiment was carried out in triplicate to ensure reliability.[27]

3.5.1. Cell line and culture conditions. The MCF-7 cell line (RRID: CVCL_0031) was obtained from the National Centre for Cell Science (NCCS), Pune, India. The cells were grown in Dulbecco's Modified Eagle's medium (DMEM) supplemented with 10% FBS, 100 U mL^{-1} penicillin, and 100 μg mL^{-1} streptomycin. The cultures were maintained at 37 °C in a humidified incubator at 5% CO_2 with 95% air. Cells were routinely subcultured every 2–3 days using 0.25% trypsin-EDTA to main-

tain them in exponential growth and ensure cellular viability throughout the study.

3.5.2. Seeding and treatment procedure. MCF-7 cells were seeded at a density of 1×10^4 cells per well in 96-well flat-bottom tissue culture plates and allowed to grow exponentially. The seeded plates were incubated for 24 h to allow adequate cell attachment before the treatment. Thereafter, the culture medium was replaced by fresh medium containing the test samples at different concentrations. The treatment groups were free TF solution prepared in 0.2% DMSO, PF127–TF micelles, and HA–PF127–TF micelles. The concentration range from 1 to 100 μg mL^{-1} for each formulation was considered, based on the drug content. In the control wells, the same volume of medium containing 0.2% DMSO was added, while untreated cells served as the negative control. Triplicate testing of each concentration was conducted to maintain statistical precision.

3.5.3. MTT assay protocol. After 24 hours of treatment exposure, 10 μL of MTT reagent at a 5 mg mL^{-1} concentration in phosphate-buffered saline was added to each well. Plates were then incubated for an additional 4 hours at 37 °C in order to allow for the mitochondrial reduction of MTT to insoluble purple formazan crystals. At the end of the incubation period, the medium containing MTT was carefully removed, and 100 μL of DMSO was added to each well in order to complete the solubilization of the formazan crystals. The absorbance of each well was measured at 570 nm using a BioTek Synergy HT microplate reader, with a reference wavelength of 630 nm used to account for background interference. The IC50 is the concentration of formulation necessary to inhibit 50% of cell viability, which was calculated by nonlinear regression analysis using GraphPad Prism version 9.0.

3.5.4. Morphological examination. The cellular morphology of MCF-7 cells was examined with an inverted phase-contrast microscope, Olympus CKX53, after 24-hour treatment. In addition, cellular morphological changes such as shrinkage, rounding, membrane blebbing, and detachment from the surface, were all typical signs of cytotoxic response. Images were captured with a high-resolution digital camera attached to the microscope in order to document various cellular morphological changes compared to untreated control cells.[27]

3.6. *In Vivo* pharmacokinetic study

The optimized HA–PF127–TF micelles were subjected to pharmacokinetic evaluation with the view of assessing the impact of micellar encapsulation and hyaluronic acid modification on its systemic bioavailability after oral administration. The study was conducted in accordance with the guidelines for the care and use of laboratory animals and was approved by the Institutional Animal Ethics Committee (IAEC), Department of Pharmaceutical Sciences, Rashtrasant Tukadoji Maharaj Nagpur University, Nagpur, Maharashtra, India (Approval No. IAEC/UDPS/2024/02/23).

3.6.1. Experimental animals. Healthy Wistar rats of either sex, weighing 200–250 g, were procured from the National Institute of Biosciences, Pune, India. The animals were housed

in polypropylene cages lined with husk under controlled environmental conditions (temperature: 25 ± 2 °C, relative humidity: 50 ± 5%, and a 12-hour light/dark cycle) with free access to a standard pellet diet and water *ad libitum*. All the animals were acclimatized under laboratory conditions one week prior to the experiment.

3.6.2. Study design. The pharmacokinetic study was performed in an open-label, randomized, parallel design. The animals were divided into two groups, each group consisting of three rats ($n = 3$). Group I received suspension of pure TF dispersed in 0.5% carboxymethyl cellulose solution, and Group II received HA–PF127–TF micelles. All formulations were orally administered through oral gavage at a dose equivalent to 10 mg kg^{-1} of Tofacitinib. Food was withheld 12 h before dosing, whereas water was provided *ad libitum*.

3.6.3. Sample collection and plasma preparation. Samples of about 0.5 mL of blood were drawn from the retro-orbital plexus of each rat at pre-defined time points of 0, 0.5, 1, 2, 4, 6, 8, 12, 24, and 48 hours post-administration. The samples were transferred into heparinized microcentrifuge tubes and centrifuged at 10 000 rpm for 10 min at 4 °C in a Remi C-24 BL refrigerated centrifuge. The separated plasma layer was collected and stored at −20 °C until further analysis.[28]

3.6.4. Plasma sample processing and drug extraction. TF was extracted from plasma by adding 100 µL of plasma to 300 µL of acetonitrile for protein precipitation. It was then vortexed for 2 minutes and centrifuged at 12 000 rpm for 10 minutes. The resultant clear supernatant was separated, filtered through a 0.22 µm syringe filter, and transferred into HPLC vials for quantification.[29]

3.6.5. Quantitative determination of tofacitinib in plasma. Quantitation of TF in rat plasma samples was made through a validated high-performance liquid chromatography (HPLC) method. TF analyses were carried out using a Shimadzu LC-20AD HPLC system fitted with an SPD-M40 photodiode array detector and a C18 reverse-phase column (4.6 × 250 mm, 5 µm). The mobile phase was 0.1% orthophosphoric acid in water/methanol (60 : 40 v/v), which was pumped through the column at a flow rate of 1.0 mL min^{-1}. The analytes were then detected at a wavelength of 287 nm using an injection volume of 20 µL. The developed analytical method was further validated for selectivity, accuracy, linearity, precision, and recovery according to ICH Q2 (R2) guidelines.[30]

3.7. Histopathological examination

Histopathological examination of tissues was carried out to check for any signs of tissue change or toxic manifestation upon oral administration of the optimized HA–Pluronic–Tofacitinib micelles compared to plain drug and non-HA micellar formulation. The animal study was performed following the CPCSEA guidelines, which deal with the purpose of controlling and supervising the conduct of experiments on animals for ensuring animal welfare and ethical research practices.

3.7.1. Experimental design and tissue collection. The animals were humanely euthanized by controlled CO_2 asphyx-

iation after the completion of the pharmacokinetic study. Immediately, major organs like liver, kidney, lungs, and heart were excised and washed with normal saline to eliminate adherent blood and tissue debris. Each organ was looked at carefully for gross pathological changes such as discoloration, swelling, or necrosis before fixation.

3.7.2. Fixation and tissue processing. The specimens were fixed in 10% neutral buffered formalin for at least 48 hours to obtain good preservation. The fixed samples were dehydrated using a gradient series of ethanol, namely, 70%, 90%, and 100%, cleared in xylene, and then embedded in paraffin wax on an automated tissue processor (Leica TP1020). The paraffin blocks were then sectioned into 4 µm thick sections using a Leica RM2235 rotary microtome.

3.7.3. Staining procedure. For demonstrating the histological architecture, the tissue sections were mounted on clean glass slides and processed for H&E staining. This was done by deparaffinization in xylene, rehydration through descending grades of alcohol, staining with Harris hematoxylin for 8 minutes, and differentiation in 1% acid alcohol. Sections were counterstained with eosin for 2 min, dehydrated in ascending grades of alcohol, cleared in xylene, and mounted with DPX mountant for observation under a microscope.

3.7.4. Microscopic examination. The stained sections were observed under a Leica DM2500 light microscope at magnification of 10×/40×. Representative photomicrographs were taken using a high-resolution digital imaging system (Leica DFC450C). Integrity of hepatic lobules, renal glomeruli, tubular epithelium, and pulmonary alveoli was observed in each treatment group. Any evidence of inflammation, necrosis, fibrosis, or cellular degeneration-a potential sign of toxicity due to formulation components-was noted with special attention.[31]

3.8. Statistical analysis

All quantitative data are presented as mean ± standard deviation (SD). Statistical analysis for *in vitro* cytotoxicity (MTT assay) was performed using one-way analysis of variance (ANOVA) followed by Tukey's multiple comparison *post hoc* test to compare differences among treatment groups. Pharmacokinetic parameters were calculated using non-compartmental analysis with Phoenix WinNonlin® software (Version 8.3, Certara, USA), and statistical comparisons between formulations were conducted using unpaired Student's *t*-test where applicable. GraphPad Prism® software (Version 9.0, GraphPad Software Inc., USA) was used for data plotting and statistical evaluation. Differences were considered statistically significant at $p < 0.05$.

4 Results and discussion

4.1. Preformulation and compatibility studies

Preformulation studies were conducted to understand the physicochemical behavior of Tofacitinib and its compatibility

with selected excipients, hyaluronic acid and Pluronic F127, for the micellar formulation.

4.1.1. Differential scanning calorimetry (DSC). A sharp endothermic melting peak appeared in the DSC thermogram of the pure TF at 208.4 °C, reflecting its crystalline nature (Fig. 3A). PF127 exhibited a broad endotherm around 58.3 °C associated with the polymeric melting transition (Fig. 3B), while HA showed a small endotherm at 112.2 °C due to the loss of bound water (Fig. 3C). All characteristic peaks were retained for the physical mixture of TF with both polymers,

with minimal shifts, indicating a lack of significant incompatibility (Fig. 3D). However, the optimized HA–PF127–TF micelles showed complete disappearance of the Tofacitinib melting peak, suggesting amorphous dispersion of the drug within the polymeric matrix. This observation confirmed successful entrapment and molecular-level solubilization of the drug within the core of the micelle.[32]

4.1.2. Fourier transform infrared spectroscopy (FTIR). In the FTIR spectrum of pure TF, the characteristic peaks were seen at 3328 cm^{-1} due to N–H stretching, 1651 cm^{-1} due to
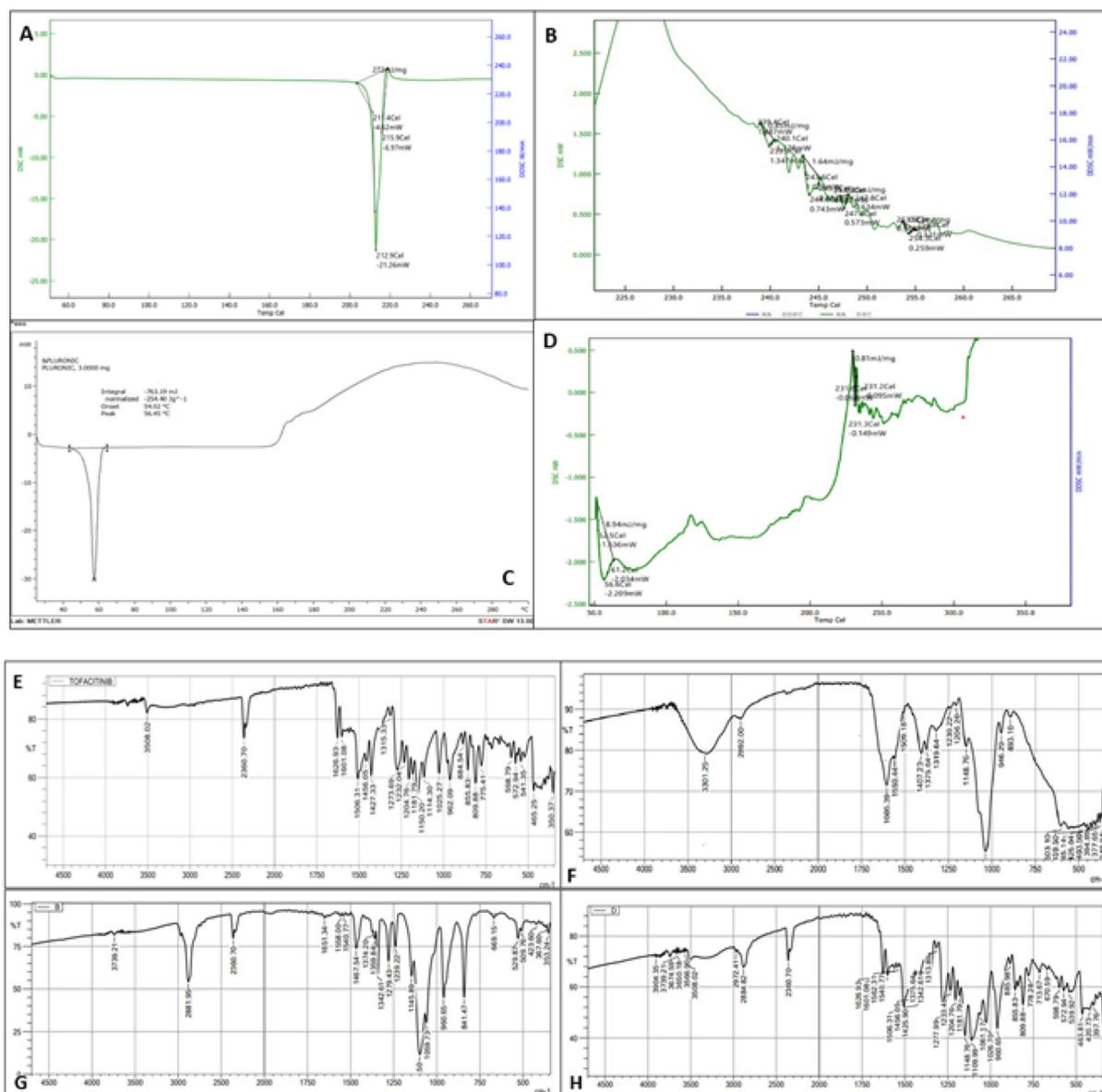

Fig. 3 Differential scanning calorimetry (DSC) thermograms of (A) pure Tofacitinib (TF), (B) pure Pluronic F127 (PF127), (C) pure Hyaluronic Acid (HA), and (D) optimized HA–PF127–TF micelles. The sharp endothermic peak of TF corresponding to its crystalline melting point is absent in the optimized micellar formulation, indicating successful amorphous dispersion and molecular encapsulation of the drug within the polymeric matrix. Fourier transform infrared (FTIR) spectra of (E) pure Tofacitinib (TF), (F) pure Hyaluronic Acid (HA), (G) pure Pluronic F127 (PF127), and (H) optimized HA–PF127–TF micelles. Characteristic absorption bands of TF, including N–H and C=O stretching vibrations, are retained in the micellar formulation without the appearance of new peaks or significant peak disappearance, indicating the absence of chemical incompatibility and confirming physical encapsulation of the drug.

C=O stretching, and 1556 cm^{-1} due to aromatic C–N stretching (Fig. 3E). The spectra of Pluronic F127 and HA showed a broad band around 3400 cm^{-1} and 1100–1150 cm^{-1} due to O–H stretching and C–O–C ether linkage, respectively (Fig. 3F and G). All the major peaks were present in the physical mixture without any appearance of new absorption bands or disappearance of existing absorption bands, proving that no chemical interaction took place. In the HA–PF127–TF micelles, small shifts of the N–H and C=O bands were evident (Fig. 3H).[14]

4.2. Formulation and optimization of HA–Pluronic–Tofacitinib micelles (QbD approach)

The formulation and optimization of HA–Pluronic–Tofacitinib micelles were performed using a systematic QbD framework based on BBD. The aim was to investigate the impact of formulation and process variables on critical micellar attributes. Three independent variables selected were drug-to-polymer ratio (A), PF127 concentration (B), and stirring temperature (C), while dependent responses were particle size (Y_1), polydispersity index (Y_2), and entrapment efficiency (Y_3).

The findings of the preformulation studies played a pivotal role in defining the critical quality attributes (CQAs) of the HA–Pluronic–Tofacitinib micellar system. DSC analysis confirmed the crystalline nature of pure tofacitinib and its conversion to an amorphous state upon micellar encapsulation, highlighting the importance of entrapment efficiency and physical stability as key CQAs. Similarly, FTIR studies demonstrated the absence of chemical incompatibility between tofacitinib and formulation excipients, supporting a formulation strategy based on physical encapsulation rather than chemical interaction. These observations underscored the necessity of controlling particle size and polydispersity index to ensure uniform drug distribution, colloidal stability, and reproducible release behavior. Consequently, particle size, PDI, entrapment efficiency, and drug release profile were selected as CQAs within the QbD framework, directly linking preformulation

insights with formulation optimization and quality risk management.

4.2.1. Model selection and statistical evaluation. A statistically appropriate quadratic model for all three responses was confirmed with low p-values (<0.05) and high coefficients of determination. Sequential model p-values and lack-of-fit results from design-expert analysis are shown in Table 3. The internal consistency of this model was justified from adjusted R^2 and predicted R^2 values for particle size, 0.8368 and −0.0547; PDI, 0.8214 and −0.1266; and entrapment efficiency, 0.8520 and 0.0803, respectively. The values of lack-of-fit were insignificant ($p > 0.05$), confirming the adequacy of the model.

$$\text{Particle size } (Y_1) = 159.2 - 6.5A - 3.875B - 12.875C \\ + 6AB\,2AC + 3.75BC + 5.525A^2 \\ + 2.775B^2 + 4.275C^2$$

$$\text{PDI } (Y_2) = 0.2214 - 0.0085A - 0.00775B - 0.016C \\ + 0.0045AB + 0.001AC + 0.0065BC \\ + 0.00855A^2 + 0.00705B^2 + 0.00405C^2$$

$$\text{Entrapment efficiency } (Y_3) = 91.14 + 2.2A + 1.5125B + 3.8375C \\ - 2.225AB + 0.525AC - 1.8BC \\ - 1.67A^2 - 0.745B^2 - 1.895C^2$$

The regression coefficients showed that factor C (stirring temperature) had the most pronounced effect throughout all the responses, followed by factor A (drug-to-polymer ratio) and factor B (PF127 concentration).

4.2.2. ANOVA summary. ANOVA showed that all response models were statistically significant ($p < 0.05$). The model F-value for particle size was 10.12, indicating a strongly significant effect of variables on the responses. Among the individual factors, C (stirring temperature) exerted the most pronounced influence with the highest F-value of 53.33. Correspondingly, the drug-to-polymer ratio, A, also showed a significant effect,

Table 3 Analysis of variance (ANOVA) results for the quadratic polynomial models of particle size, polydispersity index (PDI), and entrapment efficiency

Response	Source	Sum of squares	df	Mean square	F-value	p-Value	Significance
Particle size	Model	2263.71	9	251.52	10.12	0.0029	Significant
	A: drug-to-polymer ratio	338	1	338	13.59	0.0078	Significant
	B: PF127 concentration	120.13	1	120.13	4.83	0.0639	Moderate
	C: stirring temperature	1326.13	1	1326.13	53.33	0.00016	Highly significant
Residual	Residual	174.05	7	24.86	—	—	—
PDI	Model	0.00401	9	0.00045	9.18	0.0039	Significant
	A: drug-to-polymer ratio	0.00058	1	0.00058	11.91	0.0107	Significant
	B: PF127 concentration	0.00048	1	0.00048	9.9	0.0162	Significant
	C: stirring temperature	0.00205	1	0.00205	42.2	0.00034	Highly significant
Residual	Residual	0.00034	7	5.00×10^{-5}	—	—	—
Entrapment efficiency	Model	240.81	9	26.76	11.24	0.0021	Significant
	A: drug-to-polymer ratio	38.72	1	38.72	16.26	0.00498	Significant
	B: PF127 concentration	18.3	1	18.3	7.69	0.0276	Significant
	C: stirring temperature	117.81	1	117.81	49.47	0.0002	Highly significant
Residual	Residual	16.67	7	2.38	—	—	—

$p = 0.0077$. For PDI, the model was significant, $p = 0.0039$, with temperature, C again being the most influential variable, $F = 42.20$. Finally, the model for entrapment efficiency was very highly significant, $p = 0.0021$, and was mainly contributed by C with an F-value of 49.47, closely followed by A and B, which indicated that drug entrapment is jointly influenced by both formulation composition and process conditions.[33]

The Box–Behnken experimental design matrix, detailing the seventeen formulations generated and their corresponding observed values for particle size, PDI, and entrapment efficiency, is presented in Table 4.

4.2.3. Response interpretation and mechanistic insights. The size of the micelles fell within the range of 150–190 nm. A higher drug-to-polymer ratio A decreased the particle size up to an optimum value of 1 : 15, while higher polymer content favored micellization due to better packing of the hydrophobic core. However, higher polymer resulted in slight aggregation that increased the size. On the other hand, with the increase in the temperature of stirring in C, the particle size decreased drastically due to high kinetic energy, which favored effective self-assembly as well as evaporation of the solvent to form micelles that were more compact. Fig. 4A presents the 2D contour plots and 3D response surface plots illustrating the interactive effects of drug-to-polymer ratio, PF127 concentration, and stirring temperature on the particle size of the micelles.

PDI values of 0.21–0.26 indicated that all the formulations have a narrow size distribution. High polymer concentration with a moderate stirring temperature lowered PDI, as this improved the mobility of polymer chains. This would ensure uniform micellar nucleation. At very high concentrations, the polymers showed higher PDI values due to enhanced viscosity that interfered with proper dispersion. Fig. 4B illustrates the

2D contour plots and 3D response surface plots that depict the interaction effects of drug-to-polymer ratio, PF127 concentration, and stirring temperature on the Polydispersity Index (PDI).

The entrapment efficiency was within the range of 81–93%, and with increased drug-to-polymer ratio and higher concentration of Pluronic, there was an enhancement in EE%. This may be because of increased availability of hydrophobic domains inside the micellar core which efficiently solubilized Tofacitinib. In addition, a mild positive effect of temperature was observed probably due to improved flexibility of the polymer and swelling of micelles at elevated temperatures, thus allowing deeper incorporation of the drug.[34] Fig. 4C displays the 2D contour plots and 3D response surface plots illustrating the combined effects of drug-to-polymer ratio, surfactant concentration, and stirring temperature on the entrapment efficiency.

4.2.4 Design space optimisation and validation. In numerical optimization using the desirability function, the responses of minimum particle size, narrow PDI, and maximum EE% were pursued. Using a 1 : 15 drug to polymer (w/w) ratio, PF127 concentration of 1.0% w/v, and a stirring temperature of 40 °C, the responses for a particle size of 159.2 nm, a PDI of 0.221, and an EE% of 91.14% were predicted. Experimental validation of these showed less than a 2% prediction error, thus confirming the reliability and robustness of the established model.

In this regard, QbD-based optimization of the nanocarrier formulation showed that a well-conducted experimental design is indeed able to provide straightforward insight into the relationships among parameters and responses in such complex nanosystems. Stirring temperature (C) represents the most influential variable, which means that thermodynamic

Table 4 Experimental design matrix and observed responses. The table displays the levels of independent variables (A: drug-to-polymer ratio, B: PF127 concentration, C: stirring temperature) and the resulting dependent variables (particle size, PDI, and entrapment efficiency) for each run in the Box−Behnken design

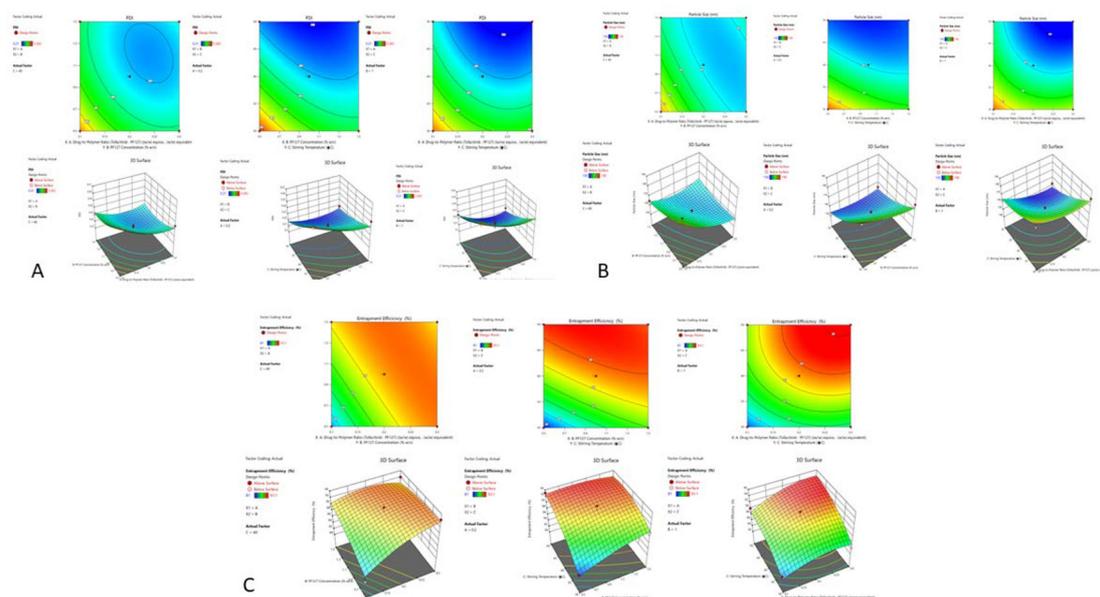|	Factors			Responses		
Run	A: drug-to-polymer ratio (tofacitinib : PF127) (%w/w) equivalent	B: PF127 concentration (% w/v)	C: stirring temperature (°C)	Particle size (nm)	PDI	Entrapment efficiency (%)
1	0.2	1.5	50	155	0.218	91.4
2	0.1	1	30	182	0.255	83.2
3	0.1	0.5	40	190	0.265	81
4	0.1	1.5	40	165	0.23	89.6
5	0.2	1	40	160	0.225	90.8
6	0.3	0.5	40	158	0.235	92.3
7	0.2	0.5	50	150	0.21	93.1
8	0.1	1	50	162	0.226	90
9	0.2	1	40	159	0.223	91
10	0.3	1	30	180	0.24	84.1
11	0.2	1	40	160	0.222	90.6
12	0.2	1	40	161	0.22	90.9
13	0.2	1.5	30	175	0.242	87.5
14	0.3	1.5	40	157	0.218	92
15	0.3	1	50	152	0.215	93
16	0.2	0.5	30	185	0.26	82
17	0.2	1	40	156	0.217	92.4

Fig. 4 Response surface analysis of micellar characteristics. The figure presents 2D contour plots (top rows) and 3D response surface plots (bottom rows) illustrating the interactive effects of independent variables—(*A*) drug-to-polymer ratio, (*B*) Pluronic F127 concentration, and (*C*) stirring temperature—on three key responses: (A) polydispersity index (PDI), (B) particle size (nm), and (C) entrapment efficiency (%). In each plot, the third variable is maintained at its midpoint.

control during micellization is the predominant factor affecting particle size and entrapment behaviour. The negative correlation of polymer concentration with both particle size and PDI suggests that micellar compaction is virtually driven by the amphiphilic re-organization of Pluronic, while HA adsorption has an ancillary role in colloidal stability. Integration of statistical modelling with mechanistic reasoning established reproducibility, reliability, and robustness as three important features for biological translation.[15]

4.3 Characterization of optimized micelles

Consequently, a QbD design-derived HA–Pluronic–Tofacitinib micellar formulation was further characterized with respect to physicochemical properties, structural morphology, thermal behaviour, and *in vitro* release performance. Characterization results showed the development of nano-sized, stable, and uniform micelles suitable for further biological evaluation.

4.3.1. Entrapment efficiency and drug loading. The optimized HA–PF127–Tofacitinib micelles had an EE % of 91.14 ± 1.8% and a DL % of 8.75 ± 0.42%, confirming the high extent of encapsulation of the hydrophobic drug inside the micellar core. The high EE could be due to the amphiphilic nature of PF127, forming a hydrophobic core, promoting the solubilization of Tofacitinib. The HA forms a hydrophilic corona providing steric stabilization. Interestingly, during the optimization process, a small increase in EE with temperature was observed, which may be due to increased mobility of the polymer chain, enabling more accommodation of drug molecules.[35]

4.3.2. Particle size, PDI and zeta potential. DLS analysis revealed an average particle size of 159.2 ± 3.8 nm with a PDI of 0.221 ± 0.015, indicating that these optimized micelles were uniformly distributed on the nanoscale (Fig. 5A). The measured zeta potential was −24.6 ± 1.2 mV, arising from the negatively charged carboxyl groups of the hyaluronic acid coating on the micelle surface (Fig. 5B). A moderately high negative zeta potential ensured colloidal stability through electrostatic repulsion, indicating successful surface modification by HA. These results are in good agreement with previously reported HA-decorated polymeric micelles, which exhibited superior circulation stability and enhanced tumor-targeting potential.

The resultant particle size of less than 200 nm supported the suitability of the formulation for passive tumor targeting *via* the enhanced permeability and retention effect. The narrow PDI confirmed homogeneity in micellar formation, one of the critical quality attributes that are important for reproducibility and stability.[36]

In addition to their targeting functionality, the HA–Pluronic nanomicelles are expected to exhibit stealth-like properties. Pluronic F127 forms a hydrophilic poly(ethylene oxide) corona around the micellar core, which is widely reported to reduce nonspecific protein adsorption and reticuloendothelial system uptake. The presence of hyaluronic acid further contributes to surface hydration and a moderately negative zeta potential, minimizing nonspecific electrostatic interactions with plasma proteins. Moreover, the optimized micelles possessed a nanoscale size below 200 nm and demonstrated prolonged systemic circulation with increased half-life and AUC, indirectly sup-
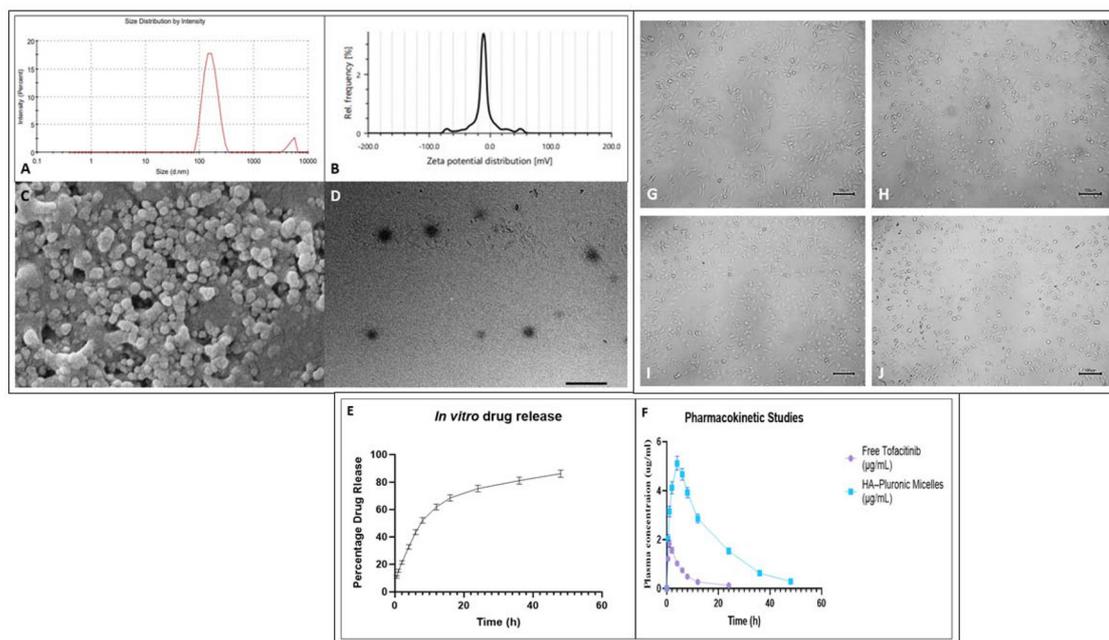
Fig. 5 The formulation was subjected to structural, morphological, and functional analysis. (A) Particle size distribution by intensity as determined by Dynamic Light Scattering (DLS). (B) Zeta potential distribution showing the surface charge of the micellar system. (C) Scanning Electron Microscopy (SEM) micrograph illustrating surface topography. (D) Transmission Electron Microscopy (TEM) image revealing the internal spherical structure and size uniformity (scale bar provided in image). (E) *In vitro* drug release profile over a 48-hour period showing the cumulative percentage of drug released. (F) Comparative pharmacokinetic profiles in plasma showing the concentration-time curve for Free Tofacitinib *versus* HA–Pluronic micelles. (G–J) Representative optical microscopy images showing cellular morphology and interaction across different experimental groups.

porting reduced clearance and stealth behavior. Collectively, these attributes suggest that the developed HA–Pluronic micelles combine passive stealth characteristics with active CD44-mediated targeting, contributing to enhanced *in vivo* performance.

4.3.3. Techniques of morphological evaluation, TEM, SEM. TEM analyses showed spherical-shaped micelles that were uniformly dispersed with smooth surfaces and no visible aggregation, as presented in Fig. 5D. Particle sizes by TEM were in agreement with DLS data, hence confirming nanoscale uniformity. SEM of the lyophilized micelles resulted in a smooth, non-porous morphology, which indicated well-formed micellar assemblies (Fig. 5C). A spherical morphology and the absence of irregularities confirmed that the thermodynamically stable formation of micelles occurred.[37]

4.3.4. *In vitro* drug release profile. The *in vitro* release profile indicated an initial burst release of *circa* 21% within the first 2 h, followed by a sustained release pattern up to 48 h with a cumulative drug release of $86.3 \pm 2.7\%$ at the end of the study (Fig. 5E). Biphasic release was attributed to drug diffusion from the outer shell (initial burst) followed by slow release from the micellar core. Kinetic modelling indicated that release followed Korsmeyer–Peppas kinetics ($R^2 = 0.984$) with a calculated 'n' value of 0.46, confirming Fickian diffusion-controlled release. The sustained release behaviour is desirable for maintaining prolonged therapeutic levels and reducing dosing frequency.

The extensive physicochemical characterization conducted proved the successful fabrication of HA–PF127–Tofacitinib micelles with optimum properties for oral and targeted drug delivery. The nanosized, monodisperse micelles proved to be colloidally stable, with high drug loading, and FTIR and DSC data confirmed compatibility and amorphous conversion. Sustained release behaviour showed effective encapsulation with diffusion-controlled release, matching the very objectives of enhancing solubility and prolonging bioavailability. The resultant properties, in particular, of size (~160 nm) and a negative surface charge are favourable for passive accumulation at tumor sites *via* the EPR effect. In addition, HA provides potential active targeting to CD44-overexpressing breast cancer cells. All the findings together justify the potential of the formulation as a repurposed nano-delivery platform for Tofacitinib in breast cancer therapy.[38]

4.4. *In vitro* cytotoxicity (MTT assay)

The MTT assay was performed with the optimized HA–Pluronic–Tofacitinib micelles against MCF-7 human breast cancer cells to investigate cytotoxic potential, as compared to free Tofacitinib and non-HA–modified Pluronic micelles. This study has been performed in order to determine the effect of nanoencapsulation and HA modification on the antiproliferative efficacy of Tofacitinib.

4.4.1. Comparative cytotoxicity analysis. The results demonstrated a concentration-dependent loss of cell viability

for all the tested formulations. Free Tofacitinib displayed relatively weak cytotoxicity with an IC_{50} value of 46.8 ± 2.4 µg mL^{-1}, which was probably due to its poor aqueous solubility and limited intracellular uptake. The non-HA–modified Pluronic–Tofacitinib micelles showed enhanced cytotoxicity and had an IC_{50} value of 28.6 ± 1.9 µg mL^{-1}, probably due to higher solubilization and better diffusivity across the cell membrane. On the contrary, HA–Pluronic–Tofacitinib micelles exhibited the highest potency, as indicated by the dramatically decreased IC_{50} value of 14.2 ± 1.1 µg mL^{-1}, confirming much higher cytotoxic efficiency ($p < 0.01$ *vs.* free drug).

The active targeting of CD44 receptors overexpressed on MCF-7 cells by HA decoration on micelles explains its enhanced cytotoxicity. HA-receptor interactions thus facilitate receptor-mediated endocytosis, which increases the internalization of drug-loaded micelles. Furthermore, improved solubilization and sustained release from the micellar core ensured higher intracellular retention of the drug and its prolonged exposure to Tofacitinib.

The reduction in IC_{50} observed for HA–Pluronic–Tofacitinib micelles was statistically significant compared with free tofacitinib and non-HA micelles ($p < 0.05$).

4.4.2. Morphological observation. The morphological changes detected in MCF-7 cells with microscopic examination after treatment clearly demonstrated distinct cytotoxic damage. Untreated control cells showed typical polygonal morphology with dense confluence, and cells treated with free Tofacitinib showed a degree of cell shrinkage with partial detachment of the cells from the bottom surface, while cells treated with HA–Pluronic–Tofacitinib micelles displayed extensive morphologic changes, including cell rounding, membrane blebbing, reduced cell density, which indicated enhanced apoptotic induction. These visual observations correlated well with the quantitative MTT data.

These findings underscore the importance of nanocarrier design for improving drug bioefficacy, as reflected by the substantial improvement in cytotoxic response following encapsulation in HA–Pluronic micelles. Besides facilitating selective uptake through CD44-mediated endocytosis, HA modification also promoted better solubility and intracellular retention of Tofacitinib. In this regard, similar observations have been made while delivering hydrophobic anticancer agents such as paclitaxel and curcumin using HA-functionalized micelles. A three-fold decrease in IC_{50} compared to free drug suggests that micellar encapsulation may potentially overcome the solubility and permeability barriers to ensure targeted cytotoxicity in models of breast cancer.

Collectively, these *in vitro* cytotoxicity results establish the superiority of HA–Pluronic–Tofacitinib micelles over free Tofacitinib and non-HA micelles in anticancer potential, thus validating the strategy of drug repurposing through targeted nanodelivery.[39]

4.5. *In vivo* pharmacokinetic evaluation

Finally, the optimized HA–Pluronic–Tofacitinib micelles were subjected to pharmacokinetic profiling in Wistar rats after oral administration, compared with free Tofacitinib and non-HA–modified Pluronic micelles, to investigate the effect of micellar encapsulation and HA surface modification on the systemic bioavailability and longevity of circulation.

4.5.1. Plasma concentration–time profile. Plasma concentration–time curves showed that there was a distinct difference in the absorption and elimination kinetics of the three groups. The free Tofacitinib suspension showed a rapid absorption phase, with C_{max} at 1.82 ± 0.14 µg mL^{-1} at $T_{max} = 1.0 \pm 0.2$ h, followed by a sharp decline, which suggested rapid systemic clearance. The Pluronic micelles with no HA modification gave C_{max} at 3.46 ± 0.22 µg mL^{-1} at $T_{max} = 2.0 \pm 0.3$ h, suggesting improved solubilization and prolonged retention. On the other hand, the HA–Pluronic–Tofacitinib micelles elicited a C_{max} as high as 5.12 ± 0.28 µg mL^{-1} with a retarded T_{max} of 4.0 ± 0.4 h, indicating an effect of sustained release with enhanced systemic absorption. In the HA-coated micellar group, the plasma concentration of Tofacitinib remained above the therapeutic threshold for more than 24 hours, while in the case of the free drug, it was reduced after just 8 hours. This prolongation in circulation time indicates efficient mucoadhesion and lymphatic uptake resistant to enzymatic degradation from the HA corona.

4.5.2. Pharmacokinetic parameters. The pharmacokinetic parameters from the non-compartmental analysis using WinNonlin 8.3 are summarized in Table 5. The $AUC_{0-\infty}$ for HA–Pluronic–Tofacitinib micelles was 96.82 ± 5.31 µg h mL^{-1}, approximately 4.3-fold higher compared with the free Tofacitinib (22.34 ± 2.85 µg h mL^{-1}). The $t_{1/2}$ increased from 3.2 ± 0.4 h for the free drug to 8.9 ± 0.7 h for HA–micelles, which indicates that there is significant reduction in the clearance rate (Table 4). The MRT was also extended from 4.1 ± 0.3 h to 10.7 ± 0.8 h, confirming sustained systemic exposure.

The pharmacokinetic results indicated that both the extent and duration of systemic exposure for the HA–Pluronic–Tofacitinib micelles were significantly improved compared with the free drug. Enhanced oral bioavailability is a result of multiple synergistic mechanisms: (i) increased solubilization of Tofacitinib within the hydrophobic micellar core, (ii) protection from enzymatic degradation due to the HA coating, (iii) mucoadhesive interaction of HA with the intestinal epi-

Table 5 Comparative pharmacokinetic parameters of free tofacitinib, Pluronic micelles, and HA–Pluronic micelles. Data are expressed as mean $\pm$ SD (n = 3). Key parameters include peak plasma concentration (C_{max}), time to peak concentration (T_{max}), area under the curve (AUC), and elimination half-life ($t_{1/2}$)

Parameter	Free tofacitinib	Pluronic micelles	HA–Pluronic micelles
C_{max} (µg mL^{-1})	1.82 ± 0.14	3.46 ± 0.22	5.12 ± 0.28
T_{max} (h)	1.0 ± 0.2	2.0 ± 0.3	4.0 ± 0.4
$AUC_{0-\infty}$ (µg h mL^{-1})	22.34 ± 2.85	54.71 ± 3.96	96.82 ± 5.31
$t_{1/2}$ (h)	3.2 ± 0.4	6.5 ± 0.6	8.9 ± 0.7
Kel (h^{-1})	0.216 ± 0.02	0.106 ± 0.01	0.078 ± 0.01
MRT (h)	4.1 ± 0.3	7.9 ± 0.5	10.7 ± 0.8
Relative bioavailability (%)	100	245	434

thelium, thus facilitating prolonged absorption, and (iv) possible lymphatic transport, thereby reducing hepatic first-pass metabolism.

Such sustained-release behavior was further confirmed by the delayed T_{max} and extended elimination half-life observed *in vitro*, which agreed with the controlled diffusion mechanism. The higher pharmacokinetic performances of HA-coated micelles reflect the trends described for HA-functionalized systems of drugs such as doxorubicin and curcumin, which all showed enhanced systemic retention and tumor accumulation.

Overall, these results substantiated the success of the QbD-optimized HA–Pluronic micellar system in enhancing the oral bioavailability and sustaining the therapeutic plasma concentration of Tofacitinib, hence advocating for its repurposing potential in the treatment of breast cancer.[40]

Statistical comparison of pharmacokinetic parameters revealed a significant increase in AUC and half-life for HA–Pluronic–Tofacitinib micelles compared to free drug ($p < 0.05$).

4.6. Histopathological examination

Histopathological examinations were carried out to investigate the safety and toxicity at the tissue level of the HA–Pluronic–Tofacitinib micelles compared with the free drug and blank micellar formulations. Organs such as the liver, kidney, heart, and lungs were collected and examined microscopically after 14 days of repeated oral administration for potential systemic toxicity or histoarchitectural changes. To verify the systemic safety of the optimized formulation, histological examination of the lungs, liver, and kidneys was performed, as shown in Fig. 6.

4.6.1. Gross and microscopic observations. Gross morphological abnormalities, such as discoloration, edema, and necrosis, were not evident in excised organs in any treatment groups upon macroscopic examination. Microscopic examination revealed well-preserved tissue architecture in the control and HA–Pluronic–Tofacitinib micelle groups, while minor changes were evident in the free drug group, indicating lower toxicity in the nanoformulated system.

Histological sections of the liver in the control and micellar-treated groups revealed normal hepatic lobular architecture with well-defined central veins and hepatic cords. Hepatocytes were polygonal with centrally located nuclei without evidence of necrosis or fatty degeneration. Histological sections of liver specimens from the free Tofacitinib suspension-treated animals, however, exhibited mild hepatocellular vacuolation together with slight infiltration of inflammatory cells, pointing to transient hepatic stress and probably related to drug accumulation and low solubility.

Renal sections from the HA–Pluronic micelle group revealed intact glomeruli and well-preserved tubular epithelium without necrosis and interstitial inflammation. However, the free drug group evinced mild tubular dilatation with epithelial desquamation, indicating irritation of the nephrons. All these findings confirmed the renal safety of this micellar formulation and also the possibility of reducing its nephrotoxic potential by controlled drug release and enhanced bioavailability.

The lung sections showed normal alveolar structures with intact septa and no inflammatory infiltrates. There was also no pulmonary edema or congestion in the micellar-treated group, further confirming the systemic biocompatibility of the formulation.

Histopathological evaluation was performed to assess the systemic safety of the optimized HA–Pluronic–Tofacitinib
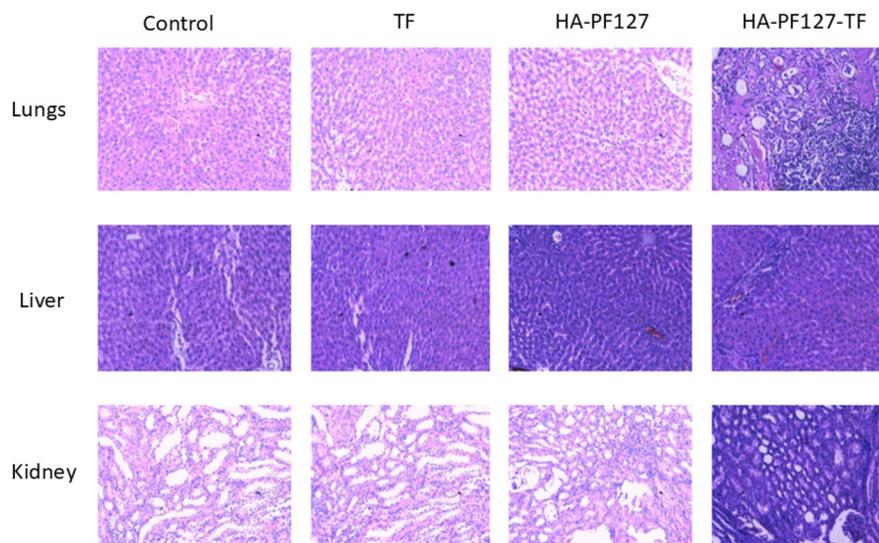

Fig. 6 Histopathological analysis of major organs *via* Hematoxylin and Eosin (H&E) staining. Representative microscopic images of lung, liver, and kidney tissues from Wistar rats treated with saline (control), free tofacitinib, blank micelles (HA–PF127), and drug-loaded micelles (HA–PF127–TF). The images demonstrate preserved tissue architecture and absence of significant pathological alterations in micelle-treated groups, indicating a favorable safety profile.

Table 6 Effect of storage conditions on the physicochemical properties of the optimized formulation. The table compares the stability of the micelles at 4 °C *versus* accelerated conditions over a 3-month period

Parameter	Initial (0 month)	1 month	2 months	3 months
Condition 4 °C				
Particle size (nm)	159.2 ± 3.8	160.3 ± 3.9	161.8 ± 4.0	162.6 ± 4.1
PDI	0.221 ± 0.015	0.224 ± 0.018	0.230 ± 0.019	0.238 ± 0.020
Zeta potential (mV)	−24.6 ± 1.2	−24.1 ± 1.3	−23.4 ± 1.4	−22.8 ± 1.5
Entrapment efficiency (%)	91.14 ± 1.8	90.47 ± 1.9	89.63 ± 2.0	88.72 ± 2.1
Condition 40 °C/75% RH				
Particle size (nm)	159.2 ± 3.8	166.5 ± 4.0	170.8 ± 4.3	175.4 ± 4.6
PDI	0.221 ± 0.015	0.246 ± 0.020	0.267 ± 0.022	0.287 ± 0.025
Zeta potential (mV)	−24.6 ± 1.2	−23.6 ± 1.4	−22.1 ± 1.6	−20.9 ± 1.8
Entrapment efficiency (%)	91.14 ± 1.8	88.56 ± 2.0	85.93 ± 2.1	83.26 ± 2.4

micelles following oral administration. Microscopic examination of hematoxylin and eosin–stained sections of liver, kidney, lung, and heart from micelle-treated animals revealed well-preserved tissue architecture comparable to the control group. Hepatic sections exhibited intact lobular organization with clearly defined central veins and hepatocyte cords, without evidence of necrosis, fatty degeneration, or inflammatory infiltration.

Renal tissues displayed normal glomerular morphology and intact tubular epithelium, with no signs of tubular dilation, epithelial desquamation, or interstitial inflammation. Pulmonary sections showed preserved alveolar architecture with thin septa and absence of edema or inflammatory cell infiltration, while cardiac tissues exhibited normal myocardial fiber arrangement without degeneration or necrosis. In contrast, animals treated with free tofacitinib showed mild, reversible histological alterations, including hepatocellular vacuolation and slight tubular changes, indicative of transient tissue stress.

Overall, these findings demonstrate that encapsulation of tofacitinib within HA–Pluronic micelles mitigates organ-level toxicity and supports the biocompatibility and systemic safety of the optimized oral nanocarrier system.[41]

4.7. Stability studies

Therefore, the optimized HA–Pluronic–Tofacitinib micelles were subjected to stability studies under accelerated and long-term conditions to determine their physicochemical integrity as well as storage suitability, according to the ICH Q1A(R2) guidelines.

4.7.1. Storage conditions and evaluation parameters. The lyophilized micelles were stored in airtight amber glass vials at two conditions:

• Long-term stability: 4 ± 2 °C (refrigerated condition)

• Accelerated stability: 40 ± 2 °C/75 ± 5% RH (environmental chamber)

During this time, samples were periodically withdrawn at 0, 1, 2, and 3 months and analyzed for particle size, PDI, zeta potential, drug content, and EE%. The physical stability of the NPs was also inspected visually for color changes, precipitation, or aggregation.

4.7.2. Physicochemical stability analysis. A marginal increase of particle size from 159.2 ± 3.8 nm to 162.6 ± 4.1 nm was observed in micelles stored at 4 °C for a period of 3 months, proving excellent physicochemical stability. PDI remained below 0.25, indicating maintained homogeneity. The zeta potential decreased slightly from −24.6 mV to −22.8 mV, still ensuring electrostatic stability. Entrapment efficiency decreased from 91.14 ± 1.8% to 88.72 ± 2.1%, which indicated negligible leakage of the drug.

Under accelerated conditions, particle size increased more 159.2 → 175.4 nm with a moderate increase in PDI 0.221 → 0.287 and slight reduction in EE 91.14 → 83.26% and zeta potential −24.6 → −20.9 mV. Yet, no significant aggregation and color change were observed, which revealed that at least for a period of 3 months the micellar formulation was stable under both conditions (Table 6).

The stability profile indeed showed that HA–Pluronic–Tofacitinib micelles exhibited excellent stability in storage at refrigerated conditions, and acceptable quality attributes were maintained under accelerated conditions. Minor increases in particle size and PDI would be expected as a function of polymer relaxation and hydration with time. Slight losses in zeta potential and EE could also arise from surface rearrangement and limited diffusion of drug through the hydrated polymeric shell.

These observations are in agreement with the previously reported stability data of Pluronic-based micellar systems, where storage at 4 °C effectively preserved the micellar integrity and drug content therein. The results confirm that the developed micelles are physically and chemically stable for extended storage, supporting their translational feasibility as a repurposed nanocarrier for Tofacitinib in breast cancer therapy.[42]

5. Conclusion

The present study demonstrates rational development, optimization, and evaluation of HA–Pluronic–Tofacitinib micelles as a repurposed nanocarrier system for targeted therapy against breast cancer. By using the Quality by Design approach, critical formulation and process parameters were identified and opti-

mized in a systematic way for the formulation of nanomicelles with desirable attributes, uniform size (~159 nm), narrow PDI (0.22), high entrapment efficiency (~91%), and strong colloidal stability (−24 mV).

A wide range of characterizations confirmed the successful formation of micelles, amorphous dispersion of drugs, and hydrogen bond-based stabilization within the hydrophobic core of Pluronic. The HA coating conferred additional surface stability and active targeting capability *via* uptake mediated by CD44 receptors. *In vitro* release studies evidenced a biphasic, diffusion-controlled profile, thus warranting prolonged drug availability.

The *in vitro* biological evaluation demonstrated a threefold increase in cytotoxicity against MCF-7 breast cancer cells compared to the free drug, confirming improved intracellular uptake and retention. A pharmacokinetic study confirmed 4.3-fold increased bioavailability but also extended half-life and delayed T_{max}, proving the potential of the formulation for prolonging systemic circulation and improving therapeutic exposure. Besides that, histopathological examination confirmed its biocompatibility and safety to organs, establishing that HA–Pluronic micelles may mitigate systemic toxicity associated with Tofacitinib.

However, from a translational perspective, this study also offers drug repurposing through nanocarrier-based delivery as a means to extend the range of applications for clinically approved molecules, such as Tofacitinib. The dual-functional approach for enhanced solubility and active targeting positions HA–Pluronic micelles as a promising oral nanoplatform in the management of breast cancer.

It should be noted that the pharmacokinetic study was conducted with a limited sample size ($n = 3$), which represents a limitation of the present work. Although the observed improvements in oral bioavailability and systemic exposure were substantial, future studies involving larger animal cohorts are required to confirm these findings and support further translational development.

Author contributions

Suchita Waghmare: writing original draft; Rohini Palekar: editing original manuscript; Pratiksha Bramhe: diagram preparation; Nilesh Rarokar: results interpretation; Pramod Khedekar: supervision.

Conflicts of interest

There is no conflict to declare.

Data availability

The data supporting this article have been included as part of the supplementary information (SI). The supplementary file consists of information regarding design expert parameters for optimization of micelles. Supplementary information is available. See DOI: https://doi.org/10.1039/d5pm00391a.

References

1 J. Kim, A. Harper, V. McCormack, H. Sung, N. Houssami, E. Morgan, *et al.*, Global patterns and trends in breast cancer incidence and mortality across 185 countries, *Nat. Med.*, 2025, **31**(4), 1154–1162. Available from: https://www.nature.com/articles/s41591-025-03502-3.

2 A. Jadhav and K. Nagaraj, Surfactant-Enabled Nanocarriers in Breast Cancer Therapy: Targeted Delivery and Multidrug Resistance Reversal, *Pharmaceutics*, 2025, **17**(6), 779. Available from: https://pmc.ncbi.nlm.nih.gov/articles/PMC12197182/.

3 X. Meng, Y. Shen, H. Zhao, X. Lu, Z. Wang and Y. Zhao, Redox-manipulating nanocarriers for anticancer drug delivery: a systematic review, *J. Nanobiotechnol.*, 2024, **22**(1), 587. Available from: https://link.springer.com/article/10.1186/s12951-024-02859-w.

4 K. Bhalodi, C. Kothari and S. Butani, Next-generation cancer nanotherapeutics: Pluronic® F127 based mixed micelles for enhanced drug delivery, *Naunyn Schmiedebergs Arch. Pharmacol.*, 2024, **398**(4), 3241–3270. Available from: https://link.springer.com/article/10.1007/s00210-024-03582-x.

5 G. Mattheolabakis, L. Milane, A. Singh and M. M. Amiji, Hyaluronic acid targeting of CD44 for cancer therapy: From receptor biology to nanomedicine, *J. Drug Targeting*, 2015, **23**(7–8), 605–618. Available from: https://www.tandfonline.com/doi/pdf/10.3109/1061186X.2015.1052072.

6 P. Kesharwani, R. Chadar, A. Sheikh, W. Y. Rizg and A. Y. Safhi, CD44-Targeted Nanocarrier for Cancer Therapy, *Front. Pharmacol.*, 2022, **12**, 800481. Available from: https://www.frontiersin.org.

7 H. Zhao, Y. Wang, J. Qian, M. Yang, C. Liu, W. Xu, *et al.*, Stimulus-responsive doxorubicin-conjugated hyaluronic acid/polypyrrole nanoplatform for targeted photothermal chemotherapy of breast cancer, *Int. J. Biol. Macromol.*, 2025, **322**, 146945. Available from: https://www.sciencedirect.com/science/article/pii/S0141813025075026.

8 B. Xiao, M. K. Han, E. Viennois, L. Wang, M. Zhang, X. Si, *et al.*, Hyaluronic acid-functionalized polymeric nanoparticles for colon cancer-targeted combination chemo-

therapy, *Nanoscale*, 2015, **7**(42), 17745–17755. Available from: https://pubs.rsc.org/en/content/articlehtml/2015/nr/c5nr04831a.

9 W. Jin, Role of JAK/STAT3 Signaling in the Regulation of Metastasis, the Transition of Cancer Stem Cells, and Chemoresistance of Cancer by Epithelial–Mesenchymal Transition, *Cells*, 2020, **9**(1), 217. Available from: https://www.mdpi.com/2073-4409/9/1/217/htm.

10 M. Palmroth, K. Kuuliala, R. Peltomaa, A. Virtanen, A. Kuuliala, A. Kurttila, *et al.*, Tofacitinib Suppresses Several JAK-STAT Pathways in Rheumatoid Arthritis In Vivo and Baseline Signaling Profile Associates With Treatment Response, *Front. Immunol.*, 2021, **12**, 738481. Available from: https://www.frontiersin.org.

11 L. De Lellis, S. Veschi, N. Tinari, Z. Mokini, S. Carradori, D. Brocco, *et al.*, Drug Repurposing, an Attractive Strategy in Pancreatic Cancer Treatment: Preclinical and Clinical Updates, *Cancers*, 2021, **13**(16), 3946. Available from: https://www.mdpi.com/2072-6694/13/16/3946/htm.

12 U. S. Younis, E. Vallorz, K. J. Addison, J. G. Ledford and P. B. Myrdal, Preformulation and Evaluation of Tofacitinib as a Therapeutic Treatment for Asthma, *AAPS PharmSciTech*, 2019, **20**(5), 167. Available from: https://link.springer.com/article/10.1208/s12249-019-1377-0.

13 S. Bashir, M. Aamir, R. M. Sarfaraz, Z. Hussain, M. U. Sarwer, A. Mahmood, *et al.*, Fabrication, characterization and in vitro release kinetics of tofacitinib-encapsulated polymeric nanoparticles: a promising implication in the treatment of rheumatoid arthritis, *Int. J. Polym. Mater. Polym. Biomater.*, 2021, **70**(7), 449–458. Available from: https://www.tandfonline.com/doi/pdf/10.1080/00914037.2020.1725760.

14 M. Kuchukuntla, V. Palanivel and A. Madhubabu, Tofacitinib Citrate-loaded Nanoparticle Gel for the Treatment of Alopecia Areata: Response Surface Design, Formulation and In vitro-In vivo Characterization, *Recent Adv. Drug Delivery Formulation*, 2023, **17**(4), 314–331. Available from: https://www.benthamdirect.com/content/journals/raddf/10.2174/0126673878264814231106094853.

15 D. Tripathi, J. Kumari, K. Rathour, P. Yadav, V. Shukla and A. K. Rai, A Review on the Progress of QbD Approach in Nanosystems Optimization: Current Updates and Strategic Applications, *Lett. Drug Des. Discovery*, 2023, **21**(13), 2545–2566. Available from: https://www.benthamdirect.com/content/journals/lddd/10.2174/0115701808082569473231004110357.

16 S. Namjoshi, M. Dabbaghi, M. S. Roberts, J. E. Grice and Y. Mohammed, Quality by Design: Development of the Quality Target Product Profile (QTPP) for Semisolid Topical Products, *Pharmaceutics*, 2020, **12**(3), 287. Available from: https://www.mdpi.com/1999-4923/12/3/287/htm.

17 L. E. Kristensen, S. Danese, A. Yndestad, C. Wang, E. Nagy, I. Modesto, *et al.*, Identification of two tofacitinib subpopulations with different relative risk versus TNF inhibitors: an analysis of the open label, randomised controlled study

ORAL Surveillance, *Ann. Rheum. Dis.*, 2023, **82**(7), 901–910. Available from: https://ard.bmj.com/content/82/7/901.

18 S. Nishal, V. Jhawat, P. Phaugat and R. Dutt, In vitro characterization of tofacitinib loaded novel nanoemulgel for topical delivery for the management of rheumatic arthritis, *Drug Dev. Ind. Pharm.*, 2022, **48**(8), 374–383. Available from: https://www.tandfonline.com/doi/pdf/10.1080/03639045.2022.2119572.

19 T. S. Anirudhan, S. Varghese and V. Manjusha, Hyaluronic acid coated Pluronic F127/Pluronic P123 mixed micelle for targeted delivery of Paclitaxel and Curcumin, *Int. J. Biol. Macromol.*, 2021, **192**, 950–957. Available from: https://www.sciencedirect.com/science/article/pii/S0141813021022121.

20 L. Zhao, J. Du, Y. Duan, Y. Zang, H. Zhang, C. Yang, *et al.*, Curcumin loaded mixed micelles composed of Pluronic P123 and F68: Preparation, optimization and in vitro characterization, *Colloids Surf., B*, 2012, **97**, 101–108. Available from: https://www.sciencedirect.com/science/article/pii/S0927776512002226.

21 H. Roy, S. P. Panda, S. K. Panda, A. K. Tripathi, S. K. Srivastava, B. S. Nayak, *et al.*, N-trimethyl chitosan and tripalmitin loaded solid lipid nanoparticles of tofacitinib citrate: Characterization and *in vivo* anti-inflammatory assessment, *J. Drug Delivery Sci. Technol.*, 2023, **87**, 104789. Available from: https://www.sciencedirect.com/science/article/abs/pii/S177322472300641X.

22 Z. Daman, S. Ostad, M. Amini and K. Gilani, Preparation, optimization and in vitro characterization of stearoyl-gemcitabine polymeric micelles: A comparison with its self-assembled nanoparticles, *Int. J. Pharm.*, 2014, **468**(1–2), 142–151. Available from: https://www.sciencedirect.com/science/article/abs/pii/S037851731400249X.

23 Z. Sezgin, N. Yüksel and T. Baykara, Preparation and characterization of polymeric micelles for solubilization of poorly soluble anticancer drugs, *Eur. J. Pharm. Biopharm.*, 2006, **64**(3), 261–268. Available from: https://www.sciencedirect.com/science/article/abs/pii/S0939641106001548.

24 F. Rehan, N. Ahemad, R. A. Islam, M. Gupta, S. H. Gan and E. H. Chowdhury, Optimization and Formulation of Nanostructured and Self-Assembled Caseinate Micelles for Enhanced Cytotoxic Effects of Paclitaxel on Breast Cancer Cells, *Pharmaceutics*, 2020, **12**(10), 984. Available from: https://www.mdpi.com/1999-4923/12/10/984/htm.

25 A. Salimi, B. S. Makhmal Zadeh and M. Kazemi, Preparation and optimization of polymeric micelles as an oral drug delivery system for deferoxamine mesylate: In vitro and ex vivo studies, *Res. Pharm. Sci.*, 2019, **14**(4), 293–307. Available from: https://journals.lww.com/rips/fulltext/2019/14040/preparation_and_optimization_of_polymeric_micelles.2.aspx.

26 S. Kaewpaiboon and T. Srichana, Formulation Optimization and Stability of Polymyxin B Based on Sodium Deoxycholate Sulfate Micelles, *J. Pharm. Sci.*, 2022, **111**(8), 2249–2257. Available from: https://www.sciencedirect.com/science/article/abs/pii/S0022354922000806.

27 H. Zhang, L. Zhao, L. Chu, X. Han and G. Zhai, Preparation, optimization, characterization and cytotoxicity in vitro of Baicalin-loaded mixed micelles, *J. Colloid Interface Sci.*, 2014, **434**, 40–47. Available from: https://www.sciencedirect.com/science/article/abs/pii/S0021979714005438.

28 Z. Y. Fang, Z. X. Jun, J. Tian, S. Hu, B. X. Hong and X. Chen, Determination of teicoplanin in human plasma by reverse micelle mediated dispersive liquid-liquid microextraction with high performance liquid chromatography, *J. Chromatogr. A*, 2021, **1643**, 462058, Available from: https://www.sciencedirect.com/science/article/abs/pii/S0021967321001825.

29 K. D. Bharwad, P. A. Shah, P. S. Shrivastav and P. Singhal, Development and validation of a rapid and sensitive UPLC–MS/MS assay for the quantification of tofacitinib in human plasma, *Biomed. Chromatogr.*, 2019, **33**(4), e4458. Available from: https://doi/pdf/10.1002/bmc.4458.

30 J. E. Kim, M. Y. Park and S. H. Kim, Simple determination and quantification of tofacitinib, a JAK inhibitor, in rat plasma, urine and tissue homogenates by HPLC and its application to a pharmacokinetic study, *J. Pharm. Invest.*, 2020, **50**(6), 603–612. Available from: https://link.springer.com/article/10.1007/s40005-020-00490-z.

31 S. Vieujean, D. Laharie, A. Buisson, X. Roblin, M. Fumery, S. Nancey, *et al.*, Histological healing induced by tofacitinib in ulcerative colitis: A multicentre study, *Dig. Liver Dis.*, 2024, **56**(4), 613–621. Available from: https://www.sciencedirect.com/science/article/abs/pii/S159086582301040X.

32 S. Bashir, M. Aamir, R. M. Sarfaraz, Z. Hussain, M. U. Sarwer, A. Mahmood, *et al.*, Fabrication, characterization and in vitro release kinetics of tofacitinib-encapsulated polymeric nanoparticles: a promising implication in the treatment of rheumatoid arthritis, *Int. J. Polym. Mater. Polym. Biomater.*, 2021, **70**(7), 449–458. Available from: https://scholar.google.com/scholar_url?url=https://www.tandfonline.com/doi/pdf/10.1080/00914037.2020.1725760%3Fcasa_token%3DuTLx-im3_-gAAAAA:EOPIhrkn3tB24oTDSMGlKFMe9zLFRwQFOm_GUXL1_93TnMmurtKD-EV5LetaQFQXVA3CRf-CgF3Sig&hl=en&sa=T&oi=ucasa&ct=ucasa&ei=HoApafDkF6qy6rQP1qz4iAU&scisig=ABGrvjKWaQXptxj70J61kpP-fnFW.

33 Z. Ansarypour, J. Emami, F. Hassanzadeh, M. Aghaei, M. Minaiyan, N. M. Davies, *et al.*, Synthesis and in vitro evaluation of novel pH-triggered biocompatible folate-chondroitin sulfate-dexamethasone copolymers for delivery of tofacitinib in rheumatoid arthritis, *Res. Pharm. Sci.*, 2025, **20**(3), 316–342. Available from: https://journals.lww.com/rips/fulltext/2025/05000/synthesis_and_in_vitro_evaluation_of_novel.1.aspx.

34 Z. Eskandari, F. Kazdal, F. Bahadori and N. Ebrahimi, Quality-by-design model in optimization of PEG-PLGA nano micelles for targeted cancer therapy, *J. Drug Delivery Sci. Technol.*, 2018, **48**, 393–402. Available from: https://www.sciencedirect.com/science/article/abs/pii/S1773224718309055.

35 S. Kim, Y. Shi, J. Y. Kim, K. Park and J. X. Cheng, Overcoming the barriers in micellar drug delivery: Loading efficiency, in vivo stability, and micelle-cell interaction, *Expert Opin. Drug Delivery*, 2010, **7**(1), 49–62. Available from: https://www.tandfonline.com/doi/pdf/10.1517/17425240903380446.

36 T. K. Wei and S. Manickam, Response Surface Methodology, an effective strategy in the optimization of the generation of curcumin-loaded micelles, *Asia–Pac. J. Chem. Eng.*, 2012, **7**(Suppl. 1), S125–S133. Available from: https://doi/pdf/10.1002/apj.661.

37 R. Kanade, M. Boche and V. Pokharkar, Self-Assembling Raloxifene Loaded Mixed Micelles: Formulation Optimization, In Vitro Cytotoxicity and In Vivo Pharmacokinetics, *AAPS PharmSciTech*, 2017, **19**(3), 1105–1115. Available from: https://link.springer.com/article/10.1208/s12249-017-0919-6.

38 A. Raval, A. Parmar, A. Raval and P. Bahadur, Preparation and optimization of media using Pluronic® micelles for solubilization of sirolimus and release from the drug eluting stents, *Colloids Surf., B*, 2012, **93**, 180–187. Available from: https://www.sciencedirect.com/science/article/abs/pii/S0927776512000021.

39 Y. Duan, J. Wang, X. Yang, H. Du, Y. Xi and G. Zhai, Curcumin-loaded mixed micelles: Preparation, optimization, physicochemical properties and cytotoxicity in vitro, *Drug Delivery*, 2015, **22**(1), 50–57. Available from: https://www.tandfonline.com/doi/pdf/10.3109/10717544.2013.873501.

40 J. Zhang, J. Liu, Y. Zhao, G. Wang and F. Zhou, Plasma and cellular pharmacokinetic considerations for the development and optimization of antitumor block copolymer micelles, *Expert Opin. Drug Delivery*, 2015, **12**(2), 263–281. Available from: https://www.tandfonline.com/doi/pdf/10.1517/17425247.2014.945417.

41 H. M. Aboud, S. F. El Menshawe, N. H. Mohammed, A. S. Tulbah and A. A. Ali, Optimization and Appraisal of Nintedanib-Loaded Mixed Polymeric Micelles as a Potential Nanovector for Non-Invasive Pulmonary Fibrosis Mitigation, *Pharmaceuticals*, 2024, **17**(10), 1275. Available from: https://www.mdpi.com/1424-8247/17/10/1275/htm.

42 C. M. L. Carvalho, J. M. S. Cabral and M. R. Aires-Barros, Cutinase stability in AOT reversed micelles: system optimization using the factorial design methodology, *Enzyme Microb. Technol.*, 1999, **24**(8–9), 569–576. Available from: https://www.sciencedirect.com/science/article/abs/pii/S014102299800163X.